Photovoltaic energy balance estimation based on the building integration level

I. Lillo-Bravo [a,*], Anton Lopez-Roman [a], Sara Moreno-Tejera [a], J.M. Delgado-Sanchez [b]

[a] Department of Energy Engineering, University of Seville, Spain
[b] Department of Applied Physics I, University of Seville, Spain

ARTICLE INFO

ABSTRACT

The photovoltaic module building integration level affects the module temperature and, consequently, its output power. In this work, a methodology has been proposed to estimate the influence of the level of architectural photovoltaic integration on the photovoltaic energy balance with natural ventilation or with forced cooling systems. The developed methodology is applied for five photovoltaic module technologies (m-Si, p-Si, a-Si, CdTe, and CIGS) on four characteristic locations (Athens, Davos, Stockholm, and Würzburg). To this end, a *photovoltaic module thermal radiation parameter, PVj*, is introduced in the characterization of the PV module technology, rendering the correlations suitable for building-integrated photovoltaic (BIPV) applications, with natural ventilation or with forced cooling systems. The results show that *PVj* has a significant influence on the energy balances, according to the architectural photovoltaic integration and climatic conditions.

© 2023 The Authors. Published by Elsevier B.V. This is an open access article under the CC BY-NC-ND license (http://creativecommons.org/licenses/by-nc-nd/4.0/).

1. Introduction

The building sector is experiencing significant challenges, being one of the most important related to energy consumption and emissions [1,2]. Photovoltaic (PV), hybrid photovoltaic-solar thermal, and solar thermal technologies [3] contribute as renewable energy sources in buildings and at the same time can serve as a weather protection, thermal insulation, noise protection, daylighting, and glare control, while at the same time giving an aesthetic and modern appearance to the building envelope.

Building integrated photovoltaic (BIPV) and building attached photovoltaic (BAPV) applications [4,5] have many options of technological designs using the high potential of the building envelope, mainly roofs, windows and facades [5,6]. Fig. 1.Fig1 shiwnb

These applications try to take advantage of the synergy of comfort, energy savings, emissions reduction, and regulatory compliance. [7]. In addition, the interest in self-consumption of PV electricity from grid-connected systems in buildings is increasing among PV system owners and in the scientific community. [8].

In all cases, the module temperature has a significant influence on the PV installation performance [9]. After incident solar irradiance, module temperature has the largest influence on photovoltaic energy yield. The output power of a module depends almost linearly on the module temperature, decreasing with increasing module temperature according to the PV cell technology, expressed by its temperature coefficient, which ranges from 0.19 %/K to 0.56 %/K in commercial modules. Moreover, usually, the more solar irradiance is received on the module, the higher temperature it may achieve. Consequently, when the module receives more solar irradiance, its conversion efficiency is decreased. In addition, not only does a high temperature module reduce the energy yield, but also causes long-term damage to the module due to its degradation [10,11].

Researchers highlight the importance of displacing the module from the building envelope to improve the natural ventilation by reducing the module temperature 12–14. Nevertheless, in this approach the PV module on the building may not achieve other significant benefits such as aesthetic and modern appearance, weather protection, thermal insulation, noise protection, daylighting techniques and glare control. To solve this issue, different forced cooling systems have been proposed and collected in several research reviews that analyze its characteristics, advantages, and drawbacks [15,16]. These cooling systems could be classified as follows:

---

* Corresponding author at: Department of Energy Engineering, Camino de los Descubrimientos, s/n. 41092 Seville Spain.
E-mail address: isidorolillo@us.es (I. Lillo-Bravo).

Nomenclature

A	PV module apertura Surface área (m^2)
a	Ambient
a-Si	Amorphous silicon module technology
BAPV	Building-applied photovoltaic
BIPV	Building-integrated photovoltaic
BIPV_T	Building-integrated photovoltaic/thermal system
CdTe	Cadmium telluride module technology
CIGS	Copper gallium indium selenide module technology
G_h	Hourly global solar irradiation on the PV module plane in the hour h (Wh/m^2)
G_{NOCT}	Hourly global solar irradiation on the PV module plane at NOCT conditions (Wh/m^2)
h	Hour
hw	Wind convection heat transfer coefficient ($W/m^2 \cdot K$)
$h_{w,NOCT}$	Wind convection heat transfer coefficient at NOCT conditions ($W/m^2 \cdot K$)
i	Photovoltaic integration level i
j	Module technology j
k_{ref}	Ross coefficient for the free-standing case
m-Si	Monocrystalline silicon module technology
NOCT	At Nominal Operating Cell Temperature conditions
p	Panel/Module
PCMs	Phase Change Materials
p-Si	Polycrystalline silicon module technology
ref	Reference conditions
$T_{a,h}$	Hourly average ambient in the hour h (°C)
$T_{a,NOCT}$	Ambient temperature at NOCT conditions (°C)
$T_{p,NOCT}$	Nominal operating cell temperature for module technology j (°C)
$T_{p,i,j,h}$	Hourly average PV module temperature in the hour h, for ω_i and module technology j (°C)
$T_{p,k}$	Highest PV module temperature that allows the cooling system (°C)
$\Delta E_{1,2,j}$ (%)	Annual energy production difference between two PV modules, one at ω_2 and another one at ω_1, with natural ventilation as a percentage of the annual energy production of the PV module at ω_1 (%)

|	
$\Delta E_{cool,i,j}$ (%)	Annual energy production difference between two PV modules, one with forced cooling system and another one with natural ventilation as a percentage of the annual energy production of the PV module with natural ventilation. Both at ω_i (%)
$\Delta P_{1,2,j,h}$ (%)	Hourly average output power difference between two PV modules, one at ω_2 and another one at w1, with natural ventilation as a percentage of the hourly average output power of the PV module at ω_1 (%)
$\Delta P_{cool,i,j,h}$ (%)	Hourly average output power difference between two PV modules, one with forced cooling system and another one with natural ventilation as a percentage of the hourly average output power of the PV module with natural ventilation. Both at ω_i (%)
$\Delta P_{1,2,j,h}$ (%)	Hourly average output power difference between two PV modules, per unit surface, one at ω_2 and another one at ω_1, for the same technology j
$P_{i,j,h}$	Hourly average power prediction per square meter of the PV module in the hour h, for ω_i and module technology j (W/m^2)
$P_{cool,i,j,h}$	Hourly average PV module temperature in the hour h, for a photovoltaic integration level in building I and a PV module technology j, with cooling system (W/m^2)
PV_j	Photovoltaic module thermal radiation parameter for module technology j. (°C·m^3/W·s)
$\Delta T_{P,2,1,j,h}$	PV module temperature difference between two PV modules with technology j, one at ω_2 and another one at ω_1 (°C)
$v_{w,h}$	Hourly average wind speed on the PV module surface in the hour h (m/s)
$v_{w,NOCT}$	Hourly average wind speed on the PV module surface at NOCT conditions in the hour h (m/s)
ω_i	Building photovoltaic integration level
$\beta_{ref,i}$	Efficiency correction coefficient for temperature (°C^{-1})
$\mu_{ref,i}$	PV module efficiency at reference conditions
κ_i	Ross coefficient for the photovoltaic integration level i
$\tau\alpha_j$	Transmittance-absorptance product of the PV module glazing for the module technology j

2. a.- PV module passive cooling systems with natural ventilation.

These systems have low or no cost, are simple without moving parts, low maintenance, no energy consumption, and easy to integrate in the building. The operating temperature of the PV module, and consequently its energy production, depends on a) the local climate, such as incoming solar irradiance on the module, ambient temperature, speed and wind direction, b) the PV cell technology and c) the level of photovoltaic integration in building [17]. For designers of BIPV and BAPV systems, it would be significant to know how much annual energy is lost or gained according to the level of integration of the PV module in the building for a certain location and the module technology, with only natural ventilation.

3. b.- PV module passive cooling systems with cooling by liquid immersion, flowing film of water on the module front or use of a phase change materials (PCMs), without forced cooling.

These systems are simple, with no moving parts, with higher heat transfer rates compared to natural air cooling, forced air circulation, and forced water circulation, higher heat absorption due to

latent heating, no energy consumption, and low maintenance cost, but with low thermal conductivity in the case of PCMs, higher cost compared to natural and forced air circulation, and with the added challenge of some PCMs being toxic or corrosive. In the case of liquid immersion cooling systems, a reduction of the module efficiency is produced due to the reduction of the solar radiation on the module. This method has a greater heat dissipation than natural ventilation, but salt deposition or corrosion may occur depending on the fluid used. Fluids such as ethanol [18], water [19] and silicon oil [20] have already been tested. In the case of a flowing film of water on the module front, the module can be successfully refrigerated while keeping its surface clean at the same time. However, some disadvantages of this configuration are the water replacement requirement due to evaporation, and the energy consumption needed to pump the water film [21]. In the case of phase change materials (PCMs), the high latent heat capacity of PCMs is utilized to maintain the module at a fairly constant temperature, even in the case of semi-transparent PV module in building. [22]. This temperature depends on the thermal characteristics of the PCMs, mass, thermal exchange surface, and local climate [23–25]. Aside of those, there are other cooling systems such as photonic crystals [26] and thermoelectric effect [27], which are under exploration.
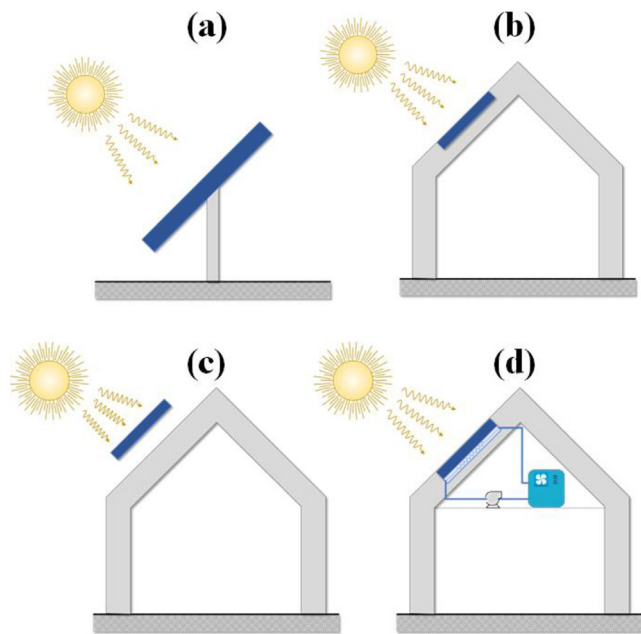
Fig. 1. Photovoltaic configurations (a) Free standing ω = 1; (b) Sloped roof with poor natural ventilation ω = 2.667; (c) Sloped roof well cooled with natural ventilation, ω = 0.952; (d) Sloped roof, with forced cooling system.

4. c.- PV module forced cooling systems.

Forced cooling systems have higher heat transfer rates compared to natural circulation, do not depend on wind conditions, have higher mass flow rates than natural air circulation and higher temperature reduction compared to natural air circulation. On the other hand, these methods have higher initial cost for fans or pumps, require ducts to handle large mass flow rates, they have operational energy consumption, high maintenance costs, can be noisy, and are difficult to integrate compared to natural air circulation system.

When considering the same contour characteristics (weather, irradiation, orientation...) for different cooling configurations, the heat dissipation required by the PV module, depends on the thermal properties of the fluid used [28], the control of the fluid flow [29], and the geometry and the surface of the thermal heat exchanger [30]. As an advantage, this type of cooling system may benefit from the thermal energy recovered, such as building integrated photovoltaic/thermal systems, (BIPV_T). [31,32].

For a correct design of cooling systems in buildings, the criteria should consider the annual energy gains, according to the cooling strategy, the range of cooling temperature of the PV module, the level of integration of the photovoltaic module in the building, the climatic conditions, and the PV module technology.

The aim of this paper is to propose a methodology to estimate these annual energy gains or losses, according to the photovoltaic integration level in the building of the modules with only natural ventilation and with forced cooling systems, depending on the climatic conditions and module technology by introducing a new module parameter called "*PV module thermal radiation parameter, PV_j*". This study considers four characteristic climatic conditions (Athens, Davos, Stockholm and Würzburg) and five PV module technologies: Monocrystalline Silicon (m-Si), Polycrystalline Silicon (p-Si), Amorphous Silicon (a-Si), Cadmium Telluride (CdTe) and Copper Indium Gallium Selenide (CIGS).

The main contributions of this article are, (i) investigating the influence of the building PV module integration level on the module temperature and its output power according to the module technology and the climatic conditions, with only natural ventila-

tion; (ii) investigating the influence of PV module forced cooling systems on the module temperature and its output power according to the building PV module integration level, to the module technology, and to the climatic conditions; and finally, (iii) analyzing the relate influence of the building PV module integration level on the PV module energy balance according to different annual climatic conditions, with and without forced cooling systems.

To the best of our knowledge, the common approaches on the estimation of the electricity production of the PV module do not separate the influence of the photovoltaic integration level in the building of the modules with only natural ventilation and with forced cooling systems, depending on the climatic conditions and module technology on the energy production. With the proposed methodology, the relative weight and influence of those factors on the electricity production can be estimated. We propose simple equations that directly allow a comparison of the influence of PV module technology and climatic conditions on the PV module temperature and power production according to the integration level of the PV module with natural ventilation.

The next part of this manuscript is organized in the following sections: Section 2 presents the methodology used to estimate the module temperature and its output power, according to the level of photovoltaic integration level in building with and without forced cooling system and the results obtained. Section 3 discusses and illustrates the photovoltaic energy balances for five PV technologies on four climate conditions. Finally, the conclusion of the paper is given in Section 4.

5. PV module output power

The level of integration of the PV module in building, with or without cooling systems, affects not only the behavior of BIPV modules as construction products, but also their electrical performance. Knowing its temperature is important for an accurate estimate of the output power of the PV module and the energy balance.

This section describes the methodology used to estimate the PV module temperature and its influence on the PV module output power for five PV module technologies (m-Si, p-Si, a-Si, CdTe, and CIGS) according to the level of building photovoltaic integration for two PV module cooling strategies. On the one hand, with only natural ventilation, and on the other hand, with forced cooling systems. The difference in annual energy production is analyzed for four climatic conditions in Section 3.

5.1. PV module output power according to the photovoltaic integration level in building with only natural ventilation.

For a module with only natural ventilation, of the relative importance of placing the module in BIPV and BAPV configuration lies on the amount of annual energy lost or gained according to the level of building photovoltaic integration and the climatic conditions.

The effect of the integration of the photovoltaic module in the building is analyzed through the parameter of building photovoltaic integration level, ω_i. This coefficient is defined as the ratio of the Ross coefficient for a photovoltaic integration level in building, k_i at hand to the Ross coefficient for the free-standing case, k_{ref}.

$$\omega_i = \frac{k_i}{k_{ref}} \tag{1}$$

Where the Ross coefficient, k_i, expresses the module temperature T_p, rise above ambient temperature, T_a with increasing global solar radiation, G_t, from t to t + Δt, for each building photovoltaic integration level, included in free-standing mode.

Table 1

Ross coefficient values and the corresponding building photovoltaic integration level.

Architectural photovoltaic integration level	k_i(K·m²·W⁻¹)	ω_i
Free standing (reference level)	k_{ref} = 0.021	1
Flat roof	0.026	1.238
Sloped roof: well cooled	0.020	0.952
Sloped roof: not so well cooled	0.034	1.619
Sloped roof: highly integrated, poorly ventilated	0.056	2.667
Facade integrated: transparent PVs	0.046	2.190
Facade integrated: opaque PVs-narrow gap	0.054	2.571

$$k = \frac{\Delta(T_p - T_a)}{\Delta(G_{t+\Delta t} - G_t)} \quad (2)$$

Table 1 shows several values of the level of building photovoltaic integration, ω_i according to equations (1) and (2), and the values of the Ross coefficient provided by Skoplaki classification. [33].

Modeling the temperature of PV modules has a long history, and many models have been presented over the years. They can be grouped as transient or steady-state models, based on whether they take the module thermal response into account (dynamic models) or assume an immediate response of the module temperature to changes in irradiance and wind speed (steady-state models) [34].

In this work, the hourly average temperature of the PV module in the hour h, for a building photovoltaic integration level ω_i and a module technology j, $T_{p,i,j,h}$ has been calculated using equation (3) [33]. This equation considers ambient temperature, solar irradiation, wind speed, integration level of the PV in building, and PV module technology. The use of this equation has been justified by Goncalves et al. [35,36] who compared simplified and detailed models for the simulation of BIPV systems with experimental measurements and concluded that "A power model combined with an empirical temperature correlation such as those of Ross and Skoplaki et al. is an option". Under steady-state (or slowly changing) conditions, $T_{p,i,j,h}$ is affected by the climatic conditions represented by the ambient temperature, wind speed, and the solar irradiation, by the level of building photovoltaic integration level represented by ω_i and by the module technology j, represented by $T_{NOCT,j}$, $\beta_{ref,j}$, $\eta_{ref,j}$ and $\tau\alpha_j$, in the following way:

$$T_{p,i,j,h} = T_{a,h} + \omega_i \cdot \left(\frac{G_h}{G_{NOCT}}\right) \cdot \frac{h_{w,NOCT}}{h_w} \cdot (T_{NOCT} - T_{a,NOCT})$$
$$\cdot \left[1 - \frac{\eta_{ref,j}}{\tau\alpha_j} \cdot \left(1 + \beta_{ref,j} \cdot T_{pref,j}\right)\right] \quad (3)$$

Where $T_{a,h}$ is the hourly average ambient temperature in the hour h expressed in °C. G_h is the hourly solar irradiation on the module plane in the hour h. $T_{NOCT,j}$ is the nominal operating cell temperature expressed in °C, $T_{pref,j}$ is the module reference temperature, $\beta_{ref,j}$ is the module power coefficient with temperature, $\eta_{ref,j}$ is the efficiency of the PV module at temperature $T_{pref,j}$ and $\tau\alpha_j$ is the module transmittance-absorptance. All these PV coefficients depend on the PV module technology "j" and their values are usually given by the module manufacturers and having average values according to the Table 2 for commercial PV modules. G_{NOCT} is the solar irradiance at nominal operating conditions, assumed 800 W/m².

Assuming $h_w = 8.91 + 2 \cdot v_{w,h}$ [33] where $v_{w,h}$ is the hourly average wind speed on the PV module surface and for wind speed in NOCT conditions of 1 m/s, results $h_{w,NOCT} = 8.91 + 2 \cdot v_{w,NOCT} = 10.91 \frac{W}{m^2 \cdot K}$. In case of special module encapsulation designs such as double glass and special designs of cooling system conducts, a detailed analyses of h_w is required ([37–39]).

A simple rearrangement in the equation (3) leads to the following expression for the module temperature:

$$T_{p,i,j,h} = T_{a,h} + \omega_i \cdot G_h \cdot (T_{NOCT,j} - 20) \cdot \left(\frac{0.0136375}{8.91 + 2 \cdot v_{w,h}}\right)$$
$$\cdot \left[1 - \frac{\eta_{ref,j}}{\tau\alpha_j} \cdot \left(1 + \beta_{ref,j} \cdot T_{pref,j}\right)\right] \quad (4)$$

Grouping the terms of equation (4) that are affected by the PV module technology "j" in the term PV_j, result equation (5):

$$PV_j = (T_{NOCT,j} - 20) \cdot 0.0136375$$
$$\cdot \left[1 - \frac{\eta_{ref,j}}{\tau\alpha_j} \cdot \left(1 + \beta_{ref,j} \cdot T_{pref,j}\right)\right] \quad (5)$$

So, the equation (4) can be rewritten as the following equation (6):

$$T_{p,i,j,h} = T_{a,h} + \omega_i \cdot PV_j \cdot \left(\frac{G_h}{8.91 + 2 \cdot v_{w,h}}\right) \quad (6)$$

Note that all the characteristics of the PV module that have an influence on the temperature of the PV module, represented by $T_{NOCT,j}$, $\beta_{ref,j}$, $\eta_{ref,j}$ and $\tau\alpha_j$, are grouped and weighted in the parameter PV_j. This parameter depends only on the PV module technology. The authors decided to called it "Photovoltaic module thermal radiation parameter". Table 3 shows the values of this parameter PV_j and other closely related parameters, such as $\beta_{ref,j}$.

Table 2

$\eta_{ref,j}$, $\beta_{ref,j}$ and $T_{NOCT,j}$ parameters from the datasheet of several manufacturers of commercial PV modules.

PV technology	Manufacturer	$\eta_{ref,j}$	$\beta_{ref,j}$ (°C⁻¹)	$T_{NOCT,j}$ (°C)	PV technology	Manufacturer	$\eta_{ref,j}$	$\beta_{ref,j}$ (°C⁻¹)	$T_{NOCT,j}$ (°C)
a-Si	QS Solar	0.06	0.0020	45	p-Si	JA Solar	0.17	0.0041	45
a-Si	Sharp	0.09	0.0024	44	p-Si	Risen Energy	0.17	0.0039	45
a-Si	Mitsubishi	0.06	0.0020	Not disclosed	p-Si	AIDU	0.17	0.0041	44
a-Si	Sharp	0.09	0.0024	44	p-Si	Indosolar	0.17	0.0043	45
a-Si	Mitsubishi	0.06	0.0020	Not disclosed	p-Si	Jetion Solar	0.17	0.0042	Not disclosed
a-Si	Merisolar	0.06	0.0020	Not disclosed	CdTe	First Solar	0.19	0.0032	Not disclosed
a-Si	Kenka	0.09	0.0035	45	CdTe	Toledo Solar	0.16	0.0033	45
a-Si	Sunwell	0.07	0.0017	Not disclosed	CdTe	Adv. Solar	0.15	0.0021	Not disclosed
a-Si	Schott Solar	0.08	0.0020	Not disclosed	CdTe	Calyxo	0.09	0.0025	40
m-Si	Astroenergy	0.22	0.0034	43	CIGS	Flisom	0.09	0.0035	Not disclosed
m-Si	Canadian S.	0.21	0.0037	43	CIGS	Solartech	0.14	0.0023	Not disclosed
m-Si	H. Q Cells	0.21	0.0035	43	CIGS	S.Frontier	0.14	0.0031	47
m-Si	Jinko Solar	0.21	0.0035	45	CIGS	DS Energy	0.18	0.0038	Not disclosed
m-Si	Longi Solar	0.21	0.0035	45	CIGS	Avancis	0.11	0.0045	56.9
m-Si	Risen Energy	0.21	0.0040	44	CIGS	Sulfurcell	0.08	0.0030	47
m-Si	Trina Solar	0.20	0.0037	44	CIGS	Wurth Solar	0.11	0.0036	47

Table 3
PV module thermal radiation parameter, PV$_j$ and other related parameters used in this work for the five discussed PV technologies.

Solar technology /reference	$T_{NOCT,j}$(°C)	$\eta_{ref,j}$	$\beta_{ref,j}$ (°C^{-1})	PV_j(°C·m^3/W·s)	$\beta_{ref,j}$·PV_j (m^3/W·s)	$\eta_{ref,j}$·$\beta_{ref,j}$·PV_j (m^3/W·s)
m-Si	43.9	0.21	0.00361	0.24302	0.000877	0.00018423
p-Si	44.8	0.17	0.00413	0.26773	0.001106	0.00018797
a-Si	44.7	0.07	0.00223	0.30919	0.000689	0.00004826
CdTe	45.0	0.13	0.00288	0.28815	0.000830	0.00010788
CIGS	49.5	0.12	0.00340	0.34411	0.001170	0.00014040

PV_j and $\eta_{ref,j}$·$\beta_{ref,j}$·PV_j. Where PV_j has been obtained from equation (5). The rest of parameters, $T_{NOCT,j}$, $\eta_{ref,j}$ and $\beta_{ref,j}$ shown in this table 3 have been obtained as the average values from the commercial PV modules, shown in the table 2, for the five PV technologies. For all the PV modules shown in table 3 have been assumed $\tau\alpha_j = 0,9$ and $T_{pref,j} = 25°$ C.

PV module temperature $T_{p,i,j,h}$ depends on the module technology by means of PV_j, on the building photovoltaic integration level by ω_i and on the climatic conditions by the ambient temperature, solar irradiation and wind speed, according to equation (6).

Although standard modules use glass for the front and a polymer for the back covers, some BIPV modules use other materials such as polymeric frontsheets, polyolefin, polyvinyl butyra, silicones, ethylene tetrafluoroethylene copolymer, polyamide, low density polyethylene, polypropylene, polyethylene terephthalate, and polyvinyl fluoride, or different types of glasses [40]. All these types of customized PV modules can be characterized using the same type of parameters than a standard module ($T_{NOCT,j}$, $\beta_{ref,j}$, $\eta_{ref,j}$ and $\tau\alpha_j$) and, consequently, would be characterized with the corresponding PV module thermal radiation parameter, PV_j using the equation (5). Consequently, equation (6) can be used for any PV module technology and any type of PV modules, custom PV module designs for BIPV included.
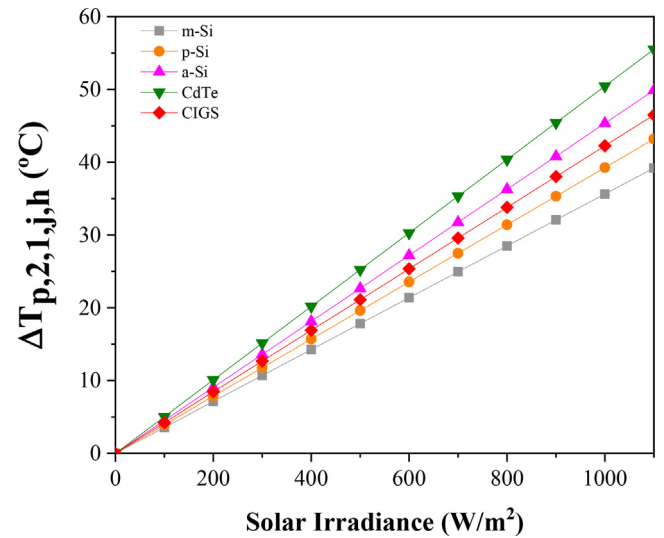
The temperature difference between two modules with the same technology, and under the same climatic conditions with only natural ventilation, but mounted with different levels of building photovoltaic integration ω_1 and ω_2, can be calculated according to equation (7).

$$\Delta T_{p,2,1,j,h} = (\omega_2 - \omega_1) \cdot PV_j \cdot \left(\frac{G_h}{8.91 + 2 \cdot v_{w,h}} \right) \quad (7)$$

Note that this difference, $\Delta T_{p,2,1,j,h}$, does not depend on ambient temperature, and the influence of PV module technology is again grouped in the term PV_j. Fig. 2 shows the difference in the temperature of the PV module for the case of $\omega_1 = 1$ and $\omega_2 = 2. 6$, and considering the five PV technologies mentioned previously, at $v_{w,h} = 1$ m/s.

Equation (7) describes the influence of the building photovoltaic integration level on its temperature. $\Delta T_{p,2,1,j,h}$ depends on the product of three factors which represent the influence of the building photovoltaic integration levels, represented by $(\omega_2 - \omega_1)$, according to the module characteristics, represented by PV_j, and for a particular climatic condition, represented by $\left(\frac{G_h}{8.91 + 2 \cdot v_{w,h}} \right)$. The strength of those factors varies with PV technologies, climatic conditions, and the level of building photovoltaic integration selected.

Fig. 2 shows that the difference in temperature of the PV module increases with irradiance up to 55 °C depending on the PV technology. Equation (7) and Fig. 2 show that module technologies with the lower temperature increase due to the increase of ω_i are those which have the lower value of PV_j. For this example, m-Si is the module technology with a lower temperature increase due to the level of building photovoltaic integration and CIGS is the one with the highest temperature increase. The values of PV_j, for

Fig. 2. PV module temperature difference between PV modules with two different building photovoltaic integration levels: $\omega_1 = 1$ and $\omega_2 = 2.6$, at.$v_{w,h} = 1$ m/s.

these two module technologies, are 0.24302 °C·m^3/W·s and 0.34411 °C·m^3/W·s respectively, according to Table 3. The higher PV_j value, the higher $\Delta T_{p,2,1,j}$ results.

The hourly average power production per square meter of the module in the hour h, for a building photovoltaic integration level ω_i and module technology j, $P_{i,j,h}$, is estimated using the equation (8) [41].

$$P_{i,j,h} = \eta_{ref,j} \cdot G_h \cdot \left[1 - \beta_{ref,j} \cdot (T_{p,i,j,h} - T_{pref,j}) \right] \quad (8)$$

Replacing $T_{p,i,j,h}$, from equation (5) in equation (8) results the following equation (9), that estimates $P_{i,j,h}$ as a function of PV_j.

$$P_{i,j,h} = \eta_{ref,j} \cdot G_h \cdot \left\{ 1 - \beta_{ref,j} \cdot \left[T_{a,h} - T_{pref,j} + \omega_i \cdot PV_j \cdot \left(\frac{G_h}{8.91 + 2 \cdot v_{w,h}} \right) \right] \right\} \approx$$

$$\approx \eta_{ref,j} \cdot G_h - \omega_i \cdot \eta_{ref,j} \cdot \beta_{ref,j} \cdot PV_j \cdot \left(\frac{G_h}{8.91 + 2 \cdot v_{w,h}} \right) \quad (9)$$

The term $T_{a,h} - T_{pref,j}$ can be considered negligible against the term $\omega_i \cdot PV_j \cdot \left(\frac{G_h}{8.91 + 2 \cdot v_{w,h}} \right)$ for all PV module technologies (See Support Information).

Thus, the output power of the photovoltaic module can be estimated as the output power of the module at reference efficiency $\eta_{ref,j} \cdot G_h$ amended by the product of three losses factors which represent the level of the building photovoltaic integration, ω_i, the module characteristics, represented by the product $\eta_{ref,j} \cdot \beta_{ref,j} \cdot PV_j$ and, the climatic conditions, represented by the expression $\frac{G_h}{8.91 + 2 \cdot v_{w,h}}$.

The hourly average output power difference between two modules, $\Delta P_{1,2,j,h}$, per unit surface, with two building photovoltaic inte-

gration levels ω_1 and ω_2, for the same module technology j, is calculated using the following equation (10).

$$\Delta P_{1,2,j,h} = P_{2,j} - P_{1,j}$$
$$= (\omega_1 - \omega_2) \cdot \eta_{ref,j} \cdot \beta_{ref,j} \cdot PV_j \cdot \left(\frac{G_h^2}{8.91 + 2 \cdot v_{w,h}} \right) \quad (10)$$

As equation (10) shows, $\Delta P_{1,2,h}$ is once again affected separately by the same factors, the building photovoltaic integration level difference, $\omega_1 - \omega_2$, the module characteristics, represented by the product $\eta_{ref,j} \cdot \beta_{ref,j} \cdot PV_j$ and, the climatic conditions by the expression $\frac{G_h^2}{8.91+2\cdot v_{w,h}}$. The a-Si module technology achieves the lowest decrease of the output power difference, while the m-Si module is the technology that achieves the highest decrease, with $\eta_{ref} \cdot \beta_{ref,j} \cdot PV_j$ equal to 0.0000482 and 0.00018423, respectively (see Table 3).

It is also of interest to know the relative difference in output power with respect to a reference building photovoltaic integration level ω_1. Thus $\Delta P_{1,2,j,h}(\%)$ provides the hourly average output power difference between two levels of building photovoltaic integration ω_1 and ω_2, as a percentage of the hourly average power production of the PV module with ω_1, according to the equation (11).

$$\Delta P_{1,2,j,h}(\%) = \frac{P_{2,j,h} - P_{1,j,h}}{P_{1,j,h}}$$
$$= \frac{(\omega_1 - \omega_2) \cdot \beta_{ref,j} \cdot PV_j \cdot \left(\frac{G_h}{8.91+2\cdot v_{w,h}} \right)}{1 - \beta_{ref,j} \cdot \left[T_{a,h} - T_{ref,j} + \omega_1 \cdot PV_j \cdot \left(\frac{G_h}{8.91+2\cdot v_{w,h}} \right) \right]} \quad (11)$$

The influence of module technology on $\Delta P_{1,2,j}(\%)$ is mainly grouped in the term $\beta_{ref,j} \cdot PV_j$, and to a lesser extent, in the term $\beta_{ref,j}$. The higher $\beta_{ref,j} \cdot PV_j$ value, the higher $\Delta P_{1,2,j}(\%)$ results.

Fig. 3 shows, $\Delta P_{1,2,j,h}(\%)$ for two building photovoltaic integration levels $\omega_1 = 1$ and $\omega_2 = 2.6$, and the five module technologies. All modules are considered at $T_{a,h} = 25\,^\circ C$ and $v_{w,h} = 1$m/s. In this example, it is observed that this percentage output power difference decreases exponentially with irradiance up to 27.4 % according to the module technology.

Fig. 3 and equation (11) show that the module technology with the lowest percentage of output power difference decrease due to
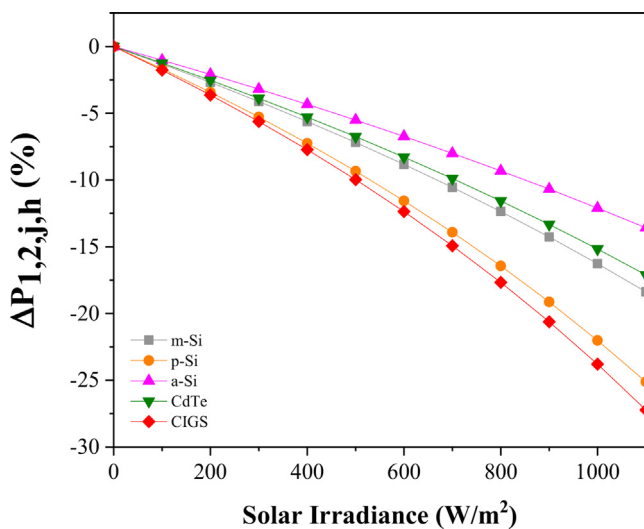

Fig. 3. Percentage output power difference between modules, with two different building photovoltaic integration levels $\omega_1 = 1$ and $\omega_2 = 2.6$, as a percentage of the power production of the module with $\omega_1 = 1$, at $T_{a,h} = 25\,^\circ C$ and $v_{w,h} = 1$m/s.

the building photovoltaic integration level is the one with the lowest value of the term $\beta_{ref,j} \cdot PV_j$. In this case, the module that has the lowest percentage loss of output power due to ω_i is a-Si and the highest percentage loss is for the CIGS technology. The $\beta_{ref,j} \cdot PV_j$ values are 0.000689 $m^3/W\cdot s$ and 0.001170 $m^3/W\cdot s$ respectively, according to Table 3.

These results demonstrate that the PV module thermal radiation parameter, PV_j, is a clear indicator of the influence of building photovoltaic integration level on the module temperature. The multiplication of this parameter by the product $\eta_{ref,j} \cdot \beta_{ref,j}$ is also a clear indicator of the influence of building photovoltaic integration level on the module output power. Moreover, PV_j multiplied by $\beta_{ref,j}$ is once again a clear indicator of the influence of building photovoltaic integration level on the PV module percentage output power. In all cases, these results refer to PV modules with natural ventilation.

5.2. PV module output power according to the building photovoltaic integration level with forced cooling system.

In addition to the analyses of the influence of the building photovoltaic integration level on the power output with only natural ventilation, the use of forced cooling systems has been studied. In this case, the main focus of this study is to seek an answer on how much annual energy is gained according to a) the PV module cooling temperature level, $T_{p,k}$ and b) building photovoltaic integration level, both depending on the climatic conditions and the module technology.

In this case, $T_{p,i,j,h}$ is the hourly average PV module temperature with natural ventilation, $T_{pcool,i,j,h}$ is the hourly average PV module temperature when there is a cooling system and $T_{p,k}$ is the highest PV module temperature allowed by the cooling system. In this work, the cooling system only works when the PV module temperature is greater than $T_{p,k}$ and $T_{a,h}$. This cooling strategy is summarized in the following expressions 12:

if $T_{p,i,j,h} > T_{p,k}$ and $T_{p,k} > T_{a,h} \gg$ then $\gg T_{pcool,i,j,h} = .T_{p,k}$
if $T_{p,i,j,h} > T_{p,k}$ and $T_{p,k} <= T_{a,h} \gg$ then $\gg T_{pcool,i,j,h}(T_{p,k}, T_{a,h}) = T_{a,h}$ (12).

if $T_{p,i,j,h} <= T_{p,k} \gg$ then $\gg T_{pcool,i,j,h} = .T_{p,i,j,h}$

We assume that the forced cooling system is able to keep the PV module temperature at $T_{p,k}$ when $T_{p,k} > T_{a,h}$.

Equation 13 is used to determine $T_{pcool,i,j,h}$ according to this strategy, where $T_{pi,j,h}$ is calculated with equation (5).

$$T_{pcool,i,j,h}(T_{p,k}, T_{a,h}, G_h, PV_j, w_i, v_{w,h})$$
$$= \frac{T_{p,k}}{4} \cdot \left\{ \left(\tanh \left[20 \cdot \left(\left(T_{a,h} + w_i \cdot \frac{PVj}{8.91+2.0 \cdot v_{w,h}} \cdot G_h \right) - T_{p,k} \right) \right] + 1 \right) \right\}$$
$$(\tanh [20 \cdot (T_{p,k} - T_{a,h})] + 1) +$$
$$+ \frac{T_{p,k}}{4} \cdot \left\{ \left(\tanh \left[20 \cdot \left(\left(T_{a,h} + w_i \cdot \frac{PVj}{8.91+2.0 \cdot v_{w,h}} \cdot G_h \right) - T_{p,k} \right) \right] + 1 \right\} (\tanh [20 \cdot (T_{p,k} - T_{a,h})] + 1) + \right.$$
$$+ \frac{T_{a,h} + w_i \frac{PVj}{8.91+2.0 \cdot vw,h} \cdot G_h}{2} \cdot \left\{ \left(\tanh \left[20 \cdot \left(\left(T_{a,h} + w_i \cdot \frac{PVj}{8.91> +2.0 \cdot v_{w,h}} \cdot G_h \right) - T_{p,k} \right) \right] + 1 \right\} \right. \quad (13).$$

Fig. 4 shows $T_{pcool,i,j,h}$ for two building photovoltaic integration levels $\omega = 1$ (left) and for $\omega = 2.6$ (right) according to the solar irradiation and ambient temperature at $T_{p,k} = 40\,^\circ C$, $v_{w,h} = 1$ m/s, and for all the PV technologies.

Fig. 4 shows that the cooling systems work more frequently when the building photovoltaic integration level, solar irradiation, and ambient temperature increases. For instance, for $\omega = 2.6$ and $T_{p,k} = 40$ °C the cooling system starts when the solar irradiance is
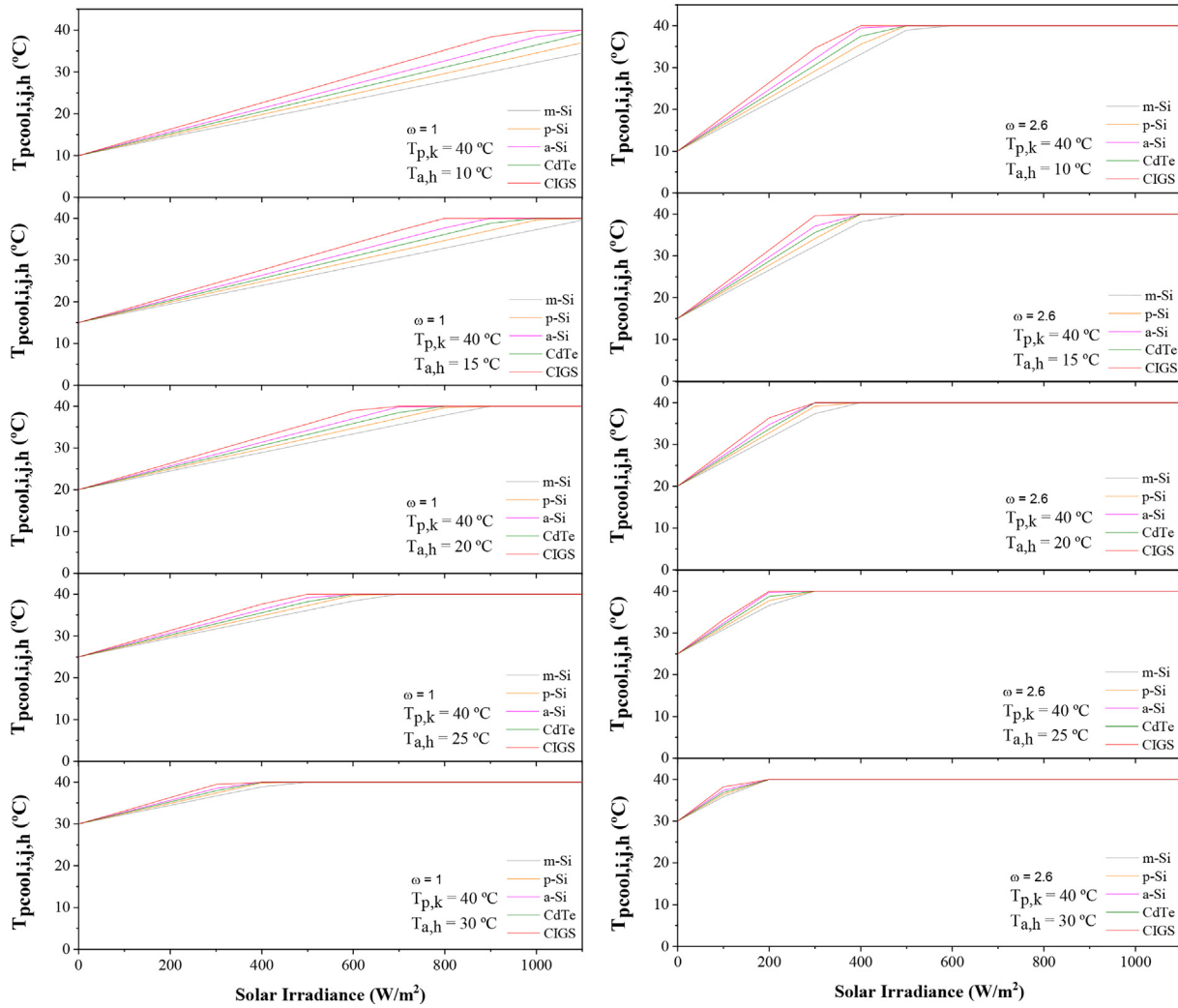
Fig. 4. PV module temperature, for $\omega = 1$ (left) and for $\omega = 2.6$ (right), according to the solar irradiation, $T_{a,h}$, and the PV technology with forced cooling systems at $T_{p,k} = 40°C$. In all cases at $v_{w,h} = 1\ m/s$.
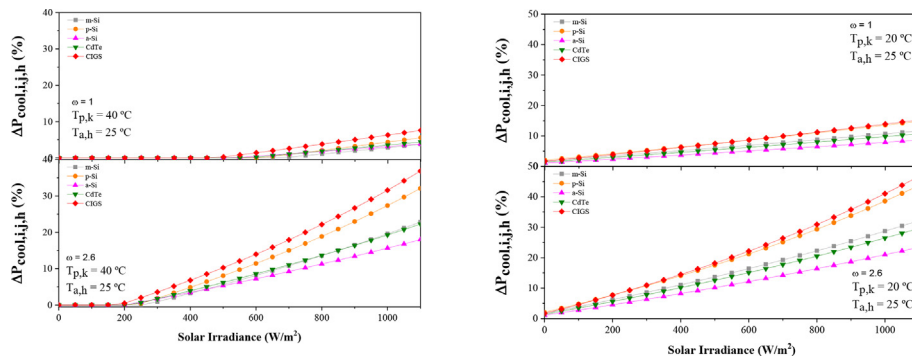

Fig. 5. - Influence of irradiance and module technology on $\Delta P_{cool,i,j,h}(\%)$, for $T_{p,k} = 40°C$ (left) and $T_{p,k} = 20°C$ (right), for $\omega_1 = 1$ and $\omega_2 = 2.6$, at $T_{a,h} = 20°C$ and $v_{w,h} = 1\ m/s$.

higher than 400 W/m^2 if $T_{a,h}$ = 10 °C, while when the ambient temperature is 30 °C, the cooling system starting level is when the solar irradiance is up to 200 W/m^2.

The hourly average output power per square meter of the module in the hour h, for a building photovoltaic integration level ω_i and the module technology j, $P_{cool,i,j,h}$ can be estimated using the equation 13 to estimate $T_{pcool,i,j,h}$, and replacing it in equation (14), similar to equation (8).

$$P_{cool,i,j,h} = \eta_{ref\,j} \cdot G_h \cdot \left[1 - \beta_{ref\,j} \cdot \left(T_{pcool,i,j,h} - T_{pref\,j}\right)\right] \qquad (14)$$

The hourly average output power difference between two modules, $\Delta P_{cool,i,j,h}$, one of them with forced cooling and the other one with only natural ventilation, is obtained through equation (15). Both under the same incident solar irradiation and with the same building photovoltaic integration level ω_i.

$$\Delta P_{cool,i,j,h} = P_{cool,i,j,h} - P_{i,j,h}$$
$$= \eta_{ref,j} \cdot \beta_{ref,j} \cdot G_h$$
$$\cdot \left[(T_{a,h} - T_{pcool,i,j,h}) + \omega_i \cdot \left(\frac{PV_j}{8,91 + 2 \cdot v_{w,h}} \right) \cdot G_h \right] \quad (15)$$

As equation (15) shows in the value of $\Delta P_{cool,i,j,h}$, the module technology is represented by the terms $\eta_{ref,j} \cdot \beta_{ref,j}$ and $\eta_{ref,j} \cdot \beta_{ref,j} \cdot PV_j$. The first one is affected by the solar irradiation and the temperature difference $(T_{a,h} - T_{pcool,i,j,h})$, and the second one is affected by the square of the solar irradiation, wind speed and the level of building photovoltaic integration.

The hourly average output power difference between a module with a cooling system and another one with only natural refrigeration can be calculated through equation (16). This equation calculates the power difference as a percentage of the hourly average power production of the module with only natural refrigeration, considering the same level of building photovoltaic integration ω_i, $\Delta P_{cool,i,j,h}(\%)$.

$$\Delta P_{cool,i,j,h}(\%) = \frac{P_{cool,i,j,h} - P_{i,j,h}}{P_{i,j,h}}$$
$$= \frac{\beta_{ref,j} \cdot \left[(T_{a,h} - T_{pcool,i,j,h}) + \omega_i \cdot PV_j \cdot \left(\frac{G_h}{8.91 + 2 \cdot v_{w,h}} \right) \right]}{1 - \beta_{ref,j} \cdot \left[(T_{a,h} - T_{ref,h}) + \omega_i \cdot PV_j \cdot \left(\frac{G_h}{8.91 + 2 \cdot v_{w,h}} \right) \right]}$$
$$(16)$$

$\Delta P_{cool,i,j,h}(\%)$ increase when $T_{p,k}$ decrease because $T_{pcool,i,j,h}$ decrease. $\Delta P_{cool,i,j,h}(\%)$ does not depend on the $\eta_{ref,j}$ and it is higher in locations with high solar irradiation levels and for PV technologies with high values of the product $\beta_{ref,j} \cdot PV_j$. Fig. 5 shows the influence of irradiance on $\Delta P_{cool,i,j,h}(\%)$ for two building photovoltaic integration levels, $\omega_1 = 1$ and $\omega_2 = 2.6$, at $T_{p,k} = 20°C$ and $T_{p,k} = 40$ °C.

Fig. 5 shows that, for low building photovoltaic integration level, the benefit of the use of a forced cooling system on the module output power is low for all PV technologies. However, when the module is highly integrated, the output power increase can reach values above 20 % – 40 %, depending on the module technology and the $T_{p,k}$ setting for the forced cooling system.

6. Energy balances

To analyze the influence of the climatic conditions on the annual percentage of the energy yield according to the photo-
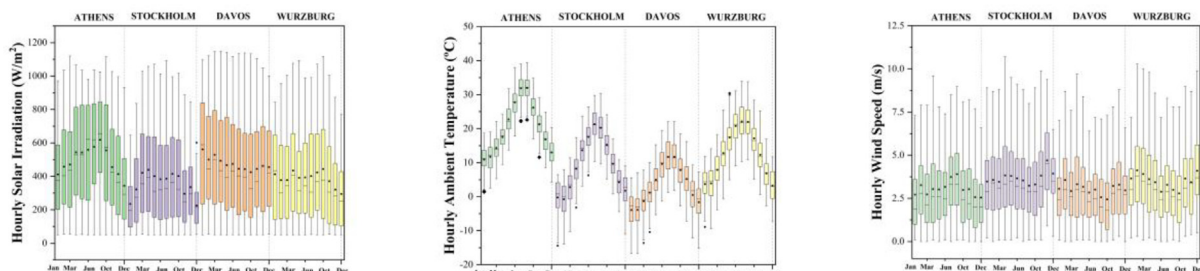
Table 4
Average climatic conditions of the selected locations.

Locations	Annual Horizontal Irradiation (kWh/m²·year)	Annual average ambient temperature (°C)
Athens	1736	18.5
Davos	1684	3.2
Würzburg	1230	9.0
Stockholm	1157	7.5

voltaic integration level in building with only natural ventilation and with forced cooling system, four locations have been selected, Athens, Davos, Stockholm and Würzburg. These locations are proposed in the EN 12976–2:2019 [41] because they represent the right combination of solar radiation and ambient temperature values, according to Table 4: Athens (high solar radiation and high ambient temperature), Davos (high solar radiation and low ambient temperature), Stockholm (low solar radiation and low ambient temperature), and Würzburg (low solar radiation and medium–low ambient temperature).

In this manuscript, the climatic data used have been the hourly average ambient temperature and wind speed and the hourly solar radiation on the plane of the PV module (sloped at the latitude of the location) provided by Meteonorm 8.0.3 climatic database. [42]. Fig. 6 shows the monthly average hourly solar irradiation, ambient temperature and wind speed for the four locations, only for the hours that there is solar irradiation. (When the irradiance on the plane of the PV module exceeds 50 W/m²).
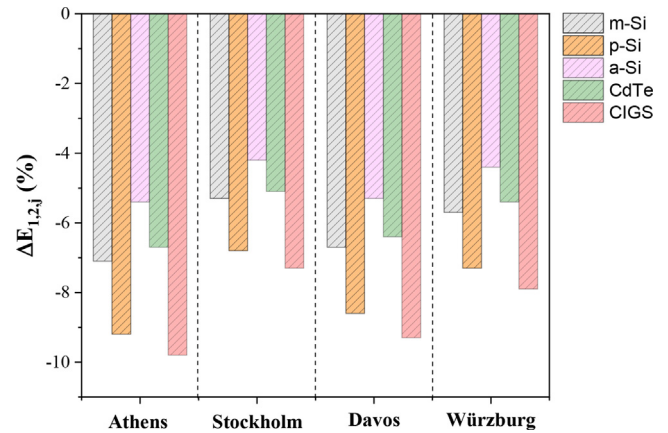
Fig. 7. Influence of the level of building integration on the annual energy percentage difference, for the five PV technologies and the four climatic conditions, at $\omega_2 = 2.6$ with respect to $\omega_1 = 1$.

Fig. 6. Monthly average hourly solar irradiation, monthly average hourly ambient temperature and monthly average hourly wind speed when solar irradiation is > 50 W/m² for the four locations.

6.1. Annual energy balance according to the building photovoltaic integration level with only natural ventilation.

The annual energy difference in the output of the PV module as a percentage of the annual energy production, per unit of surface, of the module at ω_2 with respect to another one at ω_1, $\Delta E_{1,2,j}(\%)$, has been estimated integrating the equation (11) for all hours of the year, results in the following equation (17).

$$\Delta E_{1,2,j}(\%) = \frac{(\omega_1 - \omega_2) \cdot \beta_{ref,j} \cdot PV_j \cdot \left(\sum_{h=1}^{8760} \frac{G_h}{8.91+2\cdot v_{w,h}}\right)}{\sum_{h=1}^{8760}\left(1 - \beta_{ref,j} \cdot \left[T_{a,h} - T_{ref,j,h} + \omega_1 \cdot PV_j \cdot \left(\frac{G_h}{8.91+2\cdot v_{w,h}}\right)\right]\right)}$$

$$\approx \frac{(\omega_1 - \omega_2) \cdot \beta_{ref,j} \cdot PV_j \cdot \left(\sum_{h=1}^{8760} \frac{G_h}{8.91+2\cdot v_{w,h}}\right)}{\sum_{h=1}^{8760}\left(1 - \beta_{ref,j} \cdot \left[\omega_1 \cdot PV_j \cdot \left(\frac{G_h}{8.91+2\cdot v_{w,h}}\right)\right]\right)}$$
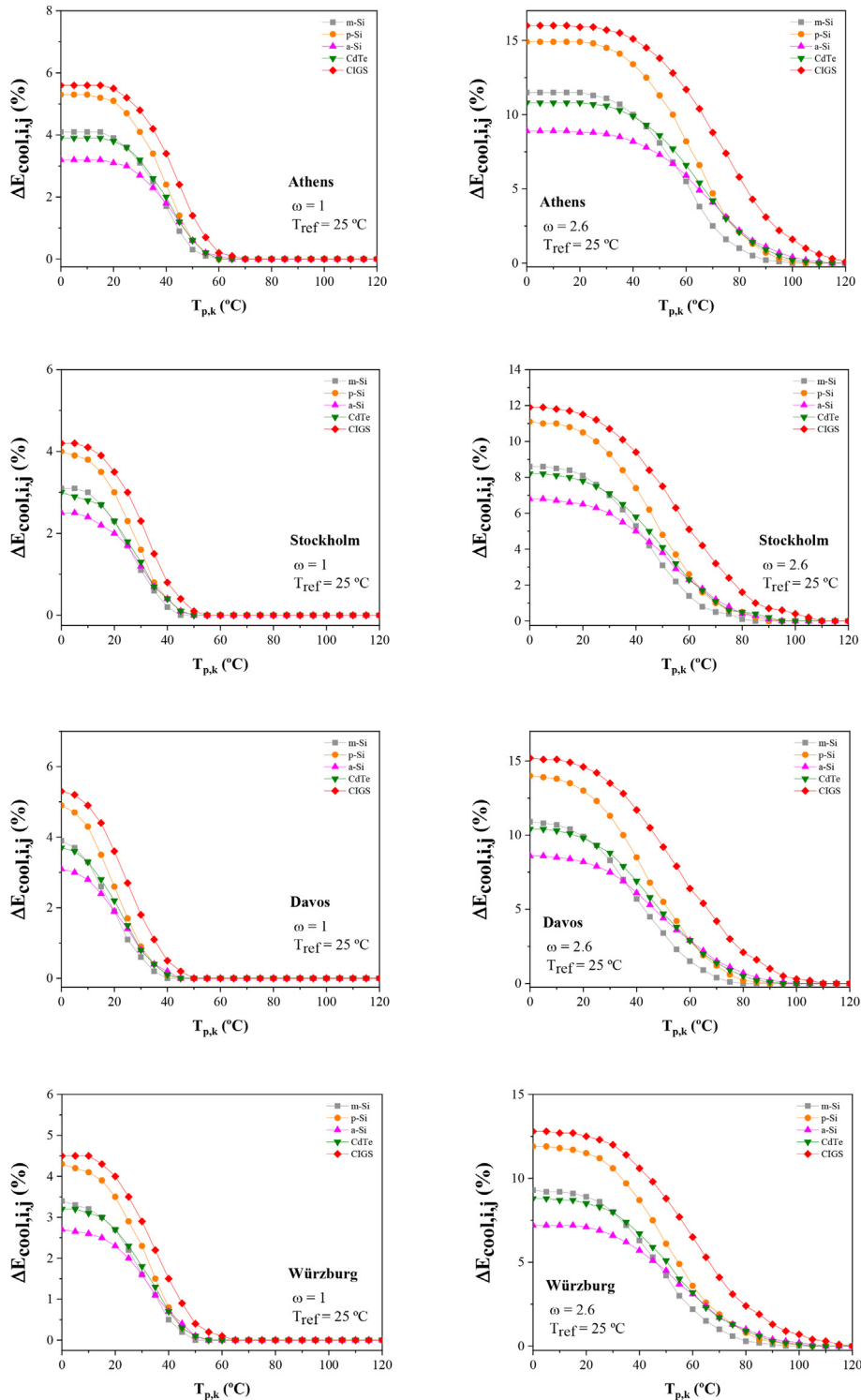
$$(17)$$

Fig. 8. $\Delta E_{cool,i,j}(\%)$ as a function of $T_{p,k}$, for the five PV module technologies, with two building integration level $w = 1$ (left) and $w = 2.6$ (right), for the four locations at $T_{p,ref} = 25$ °C.

As it can be seen, $\Delta E_{1,2,j}(\%)$ does not depend on the ambient temperature and $\eta_{ref,j}$. The higher $\beta_{ref,j} \cdot PV_j$ and G_h values, the higher $\Delta E_{1,2,j}(\%)$ results. In this case, according to the values given in Table 3, $\beta_{ref,j} \cdot PV_j$ is 0.000689 m^3/W·s for a-Si and 0.001170 m^3/W·s for CIGS, resulting that CIGS technology offers lower performance than a-Si technology, when it is mounted over an sloped roof with poor ventilation.

For instance, Fig. 7 shows the annual percentage energy difference, $\Delta E_{1,2,j}(\%)$ for the five PV technologies and the four climatic conditions, between $\omega_2 = 2.6$ and $\omega_1 = 1$, according to equation (17) and the parameters of the PV module given by Table 3 and with the values of the hourly average ambient temperature and wind speed and the hourly solar radiation on the plane of the PV module (sloped at the latitude of the location) provided by Meteonorm 8.0.3 climatic database.[42].

Note that, for a PV module technology, $\Delta E_{1,2,j}(\%)$ decreases with the solar irradiation increment, independently of ambient temperature. For this reason, locations with higher solar irradiation, in this example Athens and Davos, have the highest and similar $\Delta E_{1,2,j}(\%)$, with values among −9,1% and −5,2% for CIGS and a-Si respectively.

7. 3.2.- energy balance according to the building photovoltaic integration level with forced cooling system.

The use of a forced cooling system can reduce the PV module temperature, and consequently, the module output energy increase.

Integrating equation (16) into all hours of the year, results the following equation (18) that expresses the difference in terms of annual output energy difference between a module with forced cooling system and another one with only natural refrigeration as a percentage of the annual energy production of the module with only natural refrigeration, $\Delta E_{cool,i,j}(\%)$. In all cases with the same level of building photovoltaic integration w_i,

$$\Delta E_{cool,i,j}(\%) = \frac{\sum_{h=1}^{8760}\left[\beta_{ref,j} \cdot \left(T_{a,h} - T_{pcool,i,j,h} + w_i \cdot \left(\frac{PV_j}{8.91+2\cdot v_{w,h}}\right) \cdot G_h\right)\right]}{\sum_{h=1}^{8760}\left[1 - \beta_{ref,j} \cdot \left(T_{a,h} - T_{pref,j} + w_i \cdot \left(\frac{PV_j}{8.91+2\cdot v_{w,h}}\right) \cdot G_h\right)\right]}$$

(18)

Where, $T_{pcool,i,j,h}$ is obtained using the equation 13 for a certain temperature $T_{p,k}$.

$\Delta E_{cool,i,j}(\%)$, does not depend on $\eta_{ref,j}$, while the higher $"\beta_{ref,j} \cdot PV_j"$, $"(T_{a,h} - T_{pcool,i,j,h})"$ and $"G_h"$ values provide the higher $\Delta E_{cool,i,j}(\%)$ results.

Fig. 8 shows the influence of $T_{p,k}$ on $\Delta E_{cool,i,j}(\%)$, for the five PV technologies, with two building integration levels $w_1 = 1$ and $w_2 = 2.6$, for the four locations, at $T_{ref} = 25\,^{\circ}C$ and with the values of the hourly average ambient temperature and wind speed and the hourly solar radiation on the plane of the PV module (sloped at the latitude of the location) provided by Meteonorm 8.0.3 climatic database [41].

Fig. 8 shows that, for low building integration levels, $w_i = 1$, the influence of the forced cooling systems on $\Delta E_{cool,i,j}(\%)$ is low, between 0 for $T_{p,k}$ above 43 °C-60 °C and 5,8% for $T_{p,k}$ lower than 18 °C. The higher difference of $\Delta E_{cool,i,j}(\%)$ occurs for locations with high annual solar irradiation such as Athens. However, for high building integration levels, $w_i = 2.6$ in this case, the influence of the forced cooling systems on $\Delta E_{cool,i,j}(\%)$ is high, between 0 for high $T_{p,k}$ values and 15,6% for low $T_{p,k}$. For all locations and PV technologies, the photovoltaic increased production due to the cooling system is higher when the level of integration of the PV modules increases, with $\Delta E_{cool,i,j}(\%)$ from 2,45 % to 5,8% for $w_i = 1$ and from 7,4% to 15,44 % for $w_i = 2,6$. The selection of $T_{p,k}$ depends on loca-

tion, PV technology and integration level. There is a $T_{p,k}$ value range where $\Delta E_{cool,i,j}(\%)$ increase for each location and technology.

In all climatic conditions, $\Delta E_{cool,i,j}(\%)$ is higher for those module technologies with higher $\beta_{ref,j} \cdot PV_j$ values. In this case, Table 3 shows that the CIGS technology is the module which has the higher $\beta_{ref,j} \cdot PV_j$ value, equal to 0.001170 W/m^3·s, consistent with the results shown in the Fig. 7 for the CIGS technology.

8. Conclusions

The methodology presented in this work is able to predict the influence of the level of photovoltaic integration building on the PV module temperature, the PV module output power, and the energy yield, depending on the PV module technology selected in the design and the climatic conditions to operate.

The PV module thermal solar radiation parameter "PV_j" has been introduced. It can guide designers in their decisions to select the appropriate level of building integration of the PV modules on the roof, including the utility of using cooling systems for a location. Moreover, the products $\beta_{ref,j} \cdot PV_j$ and $\eta_{ref,j} \cdot \beta_{ref,j} \cdot PV_j$ have a clear influence on the percentage of output power of the PV module according to the building photovoltaic integration level. Using these parameters, the influence of the climatic conditions, the module technology, and the level of building integration, on the energy balance can be independently estimated.

Note that, with a limited amount of data, some of them supplied by the PV module manufacturer in the product datasheet ($\eta_{ref,j}, \beta_{ref,j}, PV_j$) and the remaining data can be taken from a climatic database ($G_h, v_{w,h}, T_{a,h}$), it could be possible to have a fast and overall estimate of the energy gained or lost due to the integration level of the PV module, ω_i.

The energy benefits of using forced cooling systems have been analyzed. The best results of using cooling systems are obtained when the module is mounting with high w_i values, the selected location has high solar irradiation, and the PV module technology selected has a high $"\beta_{ref,j} \cdot PV_j"$ value. In this case, an appropriate selection of $T_{p,k}$ is required for each module technology and climatic conditions.

Data availability

Data will be made available on request.

Declaration of Competing Interest

The authors declare that they have no known competing financial interests or personal relationships that could have appeared to influence the work reported in this paper.

References

[1] Annual Energy Outlook 2022 with projections to 2050. March, 3, 2022. U.S. Energy Information Administration. (Access online on 18th June 2022). https://www.eia.gov/outlooks/aeo/pdf/AEO2022_Narrative.pdf.

[2] S. Attia, P. Eleftheriou, F. Xeni, R. Morlot, C. Ménézo, V. Kostopoulos, M. Betsi, I. Kalaitzoglou, L. Pagliano, M. Cellura, M. Almeida, M. Ferreira, T. Baracu, V. Badescu, R. Crutescu, J.M. Hidalgo-Betanzos, Overview and future challenges of nearly zero energy buildings (nZEB) design in Southern Europe, Energy and Buildings 155 (2017) 439–458.

[3] J. Vera-Medina, M. Larrañeta, I. Lillo-Bravo, Performance of factory made solar heating systems according to standard ISO 9459–5:2007, Energy and Buildings. 183 (2019) 454–466, https://doi.org/10.1016/j.enbuild.2018.11.014.

[4] IEA. Task 41. Report. T.41.A.3/2 Task 41 - Solar Energy & Architecture - International Energy Agency- Solar Heating and Cooling Programme. Designing Photovoltaic Systems for Building Integration. Criteria and guidelines for product and system developers.2013. http://task41.iea-shc.org/Data/Sites/1/publications/task41A3-2-Designing-Photovoltaic-Systems-for-Building-Integration.pdf.

[5] E. Biyik, M. Araz, A. Hepbasli, M. Shahrestani, R. Yao, Li. Shao, E. Essah, A.C. Oliveira, T. del Caño, E. Rico, J.L. Lechón, L. Andrade, A. Mendes, Y.B. Atlı, A key review of building integrated photovoltaic (BIPV) systems, Engineering Science and Technology, an International Journal 20 (3) (2017) 833–858.

[6] T.E. Kuhn, C. Erban, M. Heinrich, J. Eisenlohr, F. Ensslen, D.H. Neuhaus, Review of technological design options for building integrated photovoltaics (BIPV), Energy and Buildings 231 (2021) 110381.

[7] A. Ghosh, Potential of building integrated and attached/applied photovoltaic (BIPV/BAPV) for adaptive less energy-hungry building's skin: A comprehensive review, Journal of Cleaner Production. 276 (2020), https://doi.org/10.1016/j.jclepro.2020.123343.

[8] A.K. Shukla, K. Sudhakar, P. Baredar, Recent advancement in BIPV product technologies: A review, Energy and Buildings 140 (2017) 188–195.

[9] I. Montero, M.T. Miranda, F. Barrena, F.J. Sepúlveda, J.I. Arranz, Analysis of photovoltaic self-consumption systems for hospitals in southwestern Europe, Energy and Buildings. 269 (2022), https://doi.org/10.1016/j.enbuild.2022.112254.

[10] G. Makrides, B. Zinsser, G.E. Georghiou, M. Schubert, J.H. Werner, Temperature behaviour of different photovoltaic systems installed in Cyprus and Germany, Solar Energy Materials and Solar Cells. 93 (6–7) (2009) 1095–1099, https://doi.org/10.1016/j.solmat.2008.12.024.

[11] P. Junsangsri, F. Lombardi, Time/Temperature Degradation of Solar Cells under the Single Diode Model, in: 2010 IEEE 25th international Symposium on Defect and Fault Tolerance in VLSI Systems (DFT, 2010, pp. 240–248.

[15] E. Kaplani, S. Kaplanis, Thermal modelling and experimental assessment of the dependence of PV module temperature on wind velocity and direction, module orientation and inclination, Solar Energy. 107 (2014) 443–460, https://doi.org/10.1016/j.solener.2014.05.037.

[16] S. Sargunanathan, A. Elango, S.T. Mohideen, Performance enhancement of solar photovoltaic cells using effective cooling methods: A review, Renewable and Sustainable Energy Reviews 64 (2016) 382–393.

[17] H. Sainthiya and N. S. Beniwal, "Different types of cooling systems used in photovoltaic module solar system: A review," 2017 International Conference on Wireless Communications, Signal Processing and Networking (WiSPNET). 2017. Pages 1500-1506. https://doi.org/10.1109/WiSPNET.2017.8300012.

[18] E. Skoplaki, J.A. Palyvos, On the temperature dependence of photovoltaic module electrical performance: A review of efficiency/power correlations, Solar Energy 83 (5) (2009) 614–624, https://doi.org/10.1016/j.solener.2008.10.008.

[19] Y. Wang, C. Wen, Q. Huang, X. Kang, M. Chen, H. Wang, Performance comparison between ethanol phase-change immersion and active water cooling for solar cells in high concentrating photovoltaic system, Energy Conversion and Management. 149 (2017) (2017) 505–513, https://doi.org/10.1016/j.enconman.2017.07.054.

[20] M. Rosa-Clot, P. Rosa-Clot, G.M. Tina, P.F. Scandura, Submerged photovoltaic solar panel: SP2, Renewable Energy 35 (8) (2010) 1862–1865.

[21] Y. Wang, Z. Fang, Li. Zhu, Q. Huang, Y. Zhang, Z. Zhang, The performance of silicon solar cells operated in liquids, Applied Energy. 86 (7-8) (2009) 1037–1042.

[22] https://doi.org/10.1016/j.apenergy.2008.08.020.

[23] S. Krauter, Increased electrical yield via water flow over the front of photovoltaic panels, Solar Energy Materials and Solar Cells. 82 (1–2) (2004) 131–137, https://doi.org/10.1016/j.solmat.2004.01.011.

[24] A. Karthick, K. Kalidasa Murugavel, A. Ghosh, K. Sudhakar, P. Ramanan, Investigation of a binary eutectic mixture of phase change material for building integrated photovoltaic (BIPV) system, Solar Energy Materials and Solar Cells 207 (2020) 110360.

[25] A. Hasan, S.J.J. McCormack, M.J.J. Huang, B. Norton, Evaluation of phase change materials for thermal regulation enhancement of building integrated photovoltaics, Solar Energy. 84 (2010) 1601–1612, https://doi.org/0.1016/j.solener.2010.06.010.

[26] Hafiz Muhammad Ali, Recent advancements in PV cooling and efficiency enhancement integrating phase change materials based systems – A comprehensive review, Solar Energy. 197 (2020) 163–198, https://doi.org/10.1016/j.solener.2019.11.075.

[27] Hao, Yu & Hong Sun, Xiao & Di Jiang, Liu & Zhang, Xu & Liang Wang, Gao. Applications of Photonic Crystals in Solar Cells. Advanced Materials Research.

Volume 760-762. 2013. Pages 281-285. https://doi.org/10.4028/www.scientific.net/AMR.760-762.281.

[28] M. Benghanem, A.A. Al-Mashraqi, K.O. Daffallah, Performance of solar cells using thermoelectric module in hot sites, Renewable Energy. 89 (2016) 51–59, https://doi.org/10.1016/j.renene.2015.12.011.

[29] F. Schiro, A. Benato, A. Stoppato, N. Destro, Improving photovoltaics efficiency by water cooling: Modelling and experimental approach, Energy. 137 (2017) 798–810, https://doi.org/10.1016/j.energy.2017.04.164.

[30] H.G. Teo, P.S. Lee, M.N.A. Hawlader, An active cooling system for photovoltaic modules, Applied Energy. 90 (2012) 309–315, https://doi.org/10.1016/j.apenergy.2011.01.017.

[31] M. Farshchimonfared, J.I. Bilbao, B.B. Sproul, Channel depth, air mass flow rate and air distribution duct diameter optimization of photovoltaic thermal (PV/T) air collectors linked to residential buildings, Renewable Energy. 76 (2015) 27–35, https://doi.org/10.1016/j.renene.2014.10.044.

[32] C. Good, J. Chen, Y. Dai, A.G. Hestnes, Hybrid Photovoltaic-thermal Systems in Buildings – A Review, Energy Procedia 70 (2015) 683–690.

[33] S. Aberoumand, S. Ghamari, B. Shabani, Energy and exergy analysis of a photovoltaic thermal (PV/T) system using nanofluids: An experimental study, Solar Energy. 165 (2018) 167–177, https://doi.org/10.1016/j.solener.2018.03.028.

[34] E. Skoplaki, A.G. Boudouvis, J.A. Palyvos, A simple correlation for the operating temperature of photovoltaic modules of arbitrary mounting, Solar Energy Materials & Solar Cells. 92 (2008) 1393–1402, https://doi.org/10.1016/j.solmat.2008.05.016.

[35] N. Martín-Chivelet, K. Kapsis, H.R. Wilson, V. Delisle, R. Yang, L. Olivieri, J. Polo, J. Eisenlohr, B. Roy, L. Maturi, G. Otnes, M. Dallapiccola, W.M.P. Upalakshi Wijeratne, Building-Integrated Photovoltaic (BIPV) products and systems: A review of energy-related behavior, Energy and Buildings 262 (2022) 111998.

[36] J.E. Gonçalves, T. van Hooff, D. Saelens, Simulating building integrated photovoltaic facades: Comparison to experimental data and evaluation of modelling complexity, Applied Energy. 281 (2021) 116032.https://doi.org/10.1016/j.apenergy.2020.116032

[37] R.A. Agathokleous, S.A. Kalogirou, Double skin facades (DSF) and building integrated photovoltaics (BIPV): A review of configurations and heat transfer characteristics, Renewable Energy. 89 (2016) 743–756, https://doi.org/10.1016/j.renene.2015.12.043.

[38] T. Baenas, M. Machado, On the analytical calculation of the solar heat gain coefficient of a BIPV module, Energy and Buildings. 151 (2017) 146–156, https://doi.org/10.1016/j.enbuild.2017.06.039.

[39] Y.B. Assoa, L. Mongibello, A. Carr, B. Kubicek, M. Machado, J. Merten, S. Misara, F. Roca, W. Sprenger, M. Wagner, S. Zamini, T. Baenas, P. Malbranche, Thermal analysis of a BIPV system by various modelling approaches, Solar Energy 155 (2017) 1289–1299.

[40] International Energy Agency Photovoltaic Power Systems Programme. IEA PVPS Task 15. Categorization of BIPV applications. Breakdown and classification of main individual parts of building skin including BIPV elements. Report IEA-PVPS T15-12:2021 August . 2021. ISBN 978-3-907281-21-5.

[41] EN 12976-2:2019. Thermal solar systems and components. Factory made systems – Part 2: Test methods.

[42] Meteonorm Software. Worldwide irradiation data. Meteonorm 8.0.3. 01/14/2021. Meteotest AG. Access on line 17th December 2022. https://meteonorm.com/en/changelog#8-0-3.

Further reading

[12] A. Omazic, G. Oreski, M. Halwachs, G.C. Eder, C. Hirschl, L. Neumaier, G. Pinter, M. Erceg, Relation between degradation of polymeric components in crystalline silicon PV module and climatic conditions: A literature review, Solar Energy Materials and Solar Cells 192 (2019) 123–133.

[13] T. Ahamed, A. Alshare, H. El-khalil, Passive cooling of building-integrated photovolatics in desert conditions: Experiment and modeling, Energy. 170 (2019) (2018) 131–1113, https://doi.org/10.1016/j.energy.2018.12.153.

[14] J.E. Gonçalves, T. van Hooff, D. Saelens, Understanding the behaviour of naturally-ventilated BIPV modules: A sensitivity analysis, Renewable Energy. 161 (2020) 133–148, https://doi.org/10.1016/j.renene.2020.06.086.